Published in final edited form as:
Epilepsia. 2013 September ; 54(9): 1668–1678. doi:10.1111/epi.12322.

7T MR spectroscopic imaging in the localization of surgical epilepsy

Jullie W. Pan[*], **Robert B. Duckrow**[†], **Jason Gerrard**[‡], **Caroline Ong**[‡], **Lawrence J. Hirsch**[†], **Stanley R. Resor Jr**[§], **Yan Zhang**[†], **Ognen Petroff**[†], **Susan Spencer**[†], **Hoby P. Hetherington**[¶], and **Dennis D. Spencer**[‡]

[*]Department of Neurology and Radiology, University of Pittsburg, Pittsburg, Pennsylvania, U.S.A.

[†]Department of Neurology, Yale University School of Medicine, New Haven, Connecticut, U.S.A.

[‡]Department of Neurosurgery, Yale University School of Medicine, New Haven, Connecticut, U.S.A.

[§]Department of Neurology, Columbia University School of Medicine, New York, New York, U.S.A.

[¶]Department of Radiology, University of Pittsburgh, Pittsburg, Pennsylvania, U.S.A.

Summary

Purpose—With the success that surgical approaches can provide for localization-related epilepsy, accurate seizure localization remains important. Although magnetic resonance (MR) spectroscopy has had success in earlier studies in medial temporal lobe epilepsy, there have been fewer studies evaluating its use in a broader range of localization-related epilepsy. With improvements in signal-to-noise with ultra-high field MR, we report on the use of high resolution 7T MR spectroscopic imaging (MRSI) in 25 surgically treated patients studied over a 3.5-year period.

Methods—Patients were included in this analysis if the region of MRSI study included the surgical resection region. Concordance between region of MRSI abnormalities and of surgical resection was classified into three groups (complete, partial, or no agreement) and outcome was dichotomized by International League Against Epilepsy (ILAE) I–III and IV–VI groups. MRSI was performed with repetition time/echo time 1.5 s/40 msec in two-dimensional (2D) or three-dimensional (3D) encoding for robust detection of singlets *N*-acetyl aspartate (NAA), creatine (Cr), and choline with abnormalities in NAA/Cr determined with correction for tissue content of gray matter.

Key Findings—The concordance between MRSI-determined abnormality and surgical resection region was significantly related to outcome: Outcome was better if the resected tissue was metabolically abnormal. All 14 patients with complete resection of the region with the most severe metabolic abnormality had good outcome, including five requiring intracranial electroencephalography (EEG) analysis, whereas only 3/11 without complete resection of the most severe metabolic abnormality had good outcome ($p < 0.001$).

Address correspondence to Jullie W. Pan, Department of Neurology, University of Pittsburgh, 3471 Fifth Avenue, Kaufmann Building 811, Pittsburgh, PA 15213, U.S.A. panjw@upmc.edu.

Disclosure

None of the authors has any conflict of interest to disclose. We confirm that we have read the Journal's position on issues involved in ethical publication and affirm that this report is consistent with those guidelines.

Significance—This is consistent with the seizure-onset zone being characterized by metabolic dysfunction and suggests that high resolution MRSI can help define these regions for the purposes of outcome prediction.

Keywords

Localization-related epilepsy; Spectroscopic imaging; Seizure localization; Outcomes

For the neurosurgical evaluation of intractable epilepsy, localization of seizure onset is a critical step. Achieving localization is commonly the result of an integrated analysis of multiple lines of evidence, including semiology, electroencephalography (EEG; scalp and intracranial), imaging, and cognitive performance. Nonetheless, the challenges of identifying seizure onset are well known, given the varying clinical expression of different brain regions and the strong possibility for rapid seizure propagation. It remains that identification with intracranial EEG data of seizure onset with accuracy that is sufficient for surgery is the goal for many magnetic resonance imaging (MRI)–negative (or MRI–ambiguous) patients. Given this, a more practical goal for improving seizure localization would be to more accurately assess candidate regions for electrode placement. In the past, MR spectroscopy and spectroscopic imaging have been suggested to be informative for localization (Connelly et al., 1994; Kuzniecky et al., 1997; Maudsley et al., 2010a); this is premised on the known role that *N*-acetyl aspartate (NAA) plays for neuronal mitochondrial function (Bates et al., 1996; Pan & Takahashi, 2005). As suggested by Connett (1988); the use of total creatine (Cr, being a key component of phosphocreatine that serves as a buffer for ATP) in the normalization of bioenergetics parameters is highly informative over a cross-section of species and within a given tissue type. Therefore, many groups have used the ratio of NAA/Cr as a normalized parameter, which we characterize as the bioenergetics of the neuronal/glial unit ("bGNU"), finding it to be informative for identifying regions of energetic and neuronal dysfunction (Suhy et al., 2000; Muñoz Maniega et al., 2008; Guevara et al., 2010).

However, MR spectroscopic imaging has been challenging (Goelman et al., 2007; Maudsley et al., 2010a,b) because of the need to cover wide brain territories, because available localization may be lobar or hemispheric. In addition, studies need to be done with sufficient spatial resolution to sensitively identify dysfunctional areas, that is, to avoid extensive partial volume effects that could otherwise dilute small abnormalities. Because of these issues, it is evident that single voxel spectroscopy is not adequate for seizure localization. With spectroscopic imaging, the technical factors of adequate signal-to-noise (SNR), consistency of coverage, and study duration have been problematic, continuing improvements in imaging technology have been made. In this report we describe the systematic use of ultra-high field (7T) MR spectroscopic imaging to evaluate seizure localization in a range of temporal and neocortical localization-related epilepsy eases. 7T is used because of the goal for high SNR in the face of relatively small voxel sizes (Vaughan et al., 2001; Inglese et al., 2006). Because of challenges intrinsic to the 7T field strength and its implementation in humans (Vaughan et al., 2001; Van de Moortele et al., 2005), this study made use of several advances in B0 shimming and radiofrequency (RF) technology to achieve consistent spectroscopic imaging performance (Avdievich et al., 2009; Hetherington et al., 2010; Pan et al., 2012a). We report on 25 patients who were included in this analysis if there was a surgical resection (rather than solely transection or device-based therapy) and there was regional overlap between the MRSI data and surgically executed plan. We assessed the concordance (complete, partial, or discordant) between the region of surgical resection and the MRSI data, and determined how this concordance related to available outcome data.

Methods

Patients

Patients were recruited by referring physicians at the Yale and Columbia Comprehensive Epilepsy Centers to participate in our 7T MR spectroscopic imaging for epilepsy study. We studied 25 patients (Table 1) from 2009 to 2012. Patients were included in this study if a surgical resection was performed, and if the preoperative MRSI data over-lapped with the surgical resection. Definition of overlap was determined from the operative note, available postoperative MRI (generally available for patients whose outcome was poor), and 7T structural imaging data. In all cases, localization and decision for surgical resection were determined by expert review and consensus opinion of the Yale or Columbia Comprehensive Epilepsy Programs and did not make explicit use of MRSI data. The MRSI studies were not performed as whole brain studies; however, as they included multiple slices and were targeted to suspected regions of interest (lobar, limbic) for seizure localization, there was minimal patient exclusion (2/27 patients who otherwise qualified) because of nonoverlap with the surgical resection. The shortest time period of follow-up was 4 months, the longest 3.5 years, with a majority of patients (20/25) with >1 year of follow-up.

Classification of patients was made based on the concordance between the MR spectroscopic imaging (MRSI) abnormalities with surgical resection. Three levels of concordance were used:

1. Complete concordance: The region of most severe NAA/Cr abnormality is resected, with or without areas of lesser MRSI abnormality.
2. Partial concordance: The region of NAA/Cr abnormality is partly resected, although there were other areas of equal or worse MRSI abnormality that were not resected.
3. Discordant: The region of NAA/Cr abnormality is not resected, that is, the surgically resected area showed no abnormality on MRSI.

Outcome was classified using the International League Against Epilepsy (LAE) scale. Because of the small number of patients studied, ILAE outcomes were dichotomized into good outcome (ILAEI–III: seizure free or up to three seizure days/year) and poor outcome (ILAEIV–VI: at least four seizure days/year). As a result, a 3 × 2 contingency table was used to compare concordance class and ILAE outcome. It should be noted in this initial study that because imaging studies were performed locally based on clinically suspected brain regions, these studies should not be regarded as “blinded” independent measurements for seizure localization.

MR spectroscopic imaging

7T MR spectroscopic imaging was performed using a head-only Agilent (Varian, Agilent Technologies, Santa Clara, CA, U.S.A.) human imaging spectrometer equipped with 40 mT/m gradients and third-order shim coils. Because of the need for excellent Bo homogeneity over large regions of the brain sufficient for spectroscopic imaging, an RRI (Resonance Research Inc., Billerica, MA, U.S.A.) high fourth-degree shim insert coil was additionally used in conjunction with map based noniterative shimming methods as described previously (Pan et al., 2012a). All studies used an eight-channel transceiver array for detection with RE shimming (Avdievich et al., 2009). Scout imaging was performed using an inversion recovery (IR) gradient echo for gray–white matter contrast (repetition time/echo time [TR/TE] 1.5 s/10 msec). Spectroscopic localization was achieved with a combination of gradient-based slice-selective excitation (10-mm thick slices) and RE shimming based outer volume suppression (Avdievich et al., 2009; Hetherington et al., 2010). MRSI studies were acquired

as Hahn spin echoes with repetition time/echo time [TR/TE] 1.5 s/40 msec with rectangular phase encoding. The voxel size did vary through the 3.5-year period of these studies, with the initial studies (n = 4) acquired at a nominal voxel size of 1.44 cc (16 × 16 phase encoding), and later studies (n = 21) at 0.64 cc (24 × 24 phase encoding). In the initiation of this study, tissue segmentation was performed manually for the neocortical studies from the scout IR gradient echo images; however, the later studies in this dataset used tissue segmentation with a calibrated inversion recovery that takes advantage of the longer T_1 values at 7T (Rooney et al., 2007). Examples of this are shown in Figures 1 and 4. The total duration of any given study was approximately 80 min.

Data were processed with 4 Hz of Gaussian broadening (full-width half maximum [FWHM]) in the spectral domain and a Hanning filter in the spatial domain. Spectra were phased and fit in the spectral domain using Gaussian line-shapes, and the ratios of NAA/Cr were calculated using resonance areas. Because of the moderate echo time (TE 40 msec) used, minimal baseline correction (performed using a cubic spline fit) was needed. As discussed by Connett (1988), the normalization with regard to total creatine has proven informative and robust for parameters of bioenergetics and metabolic function owing to the key role of creatine and phosphocreatine in buffering ATP. It should be noted that this normalization is pertinent not only bioenergetically but also renders the parameter relatively insensitive to variations in tissue atrophy and partial volume effects. The variation in NAA and creatine in white versus gray matter does result in variation in NAA/Cr, and thus evaluations for significance were corrected for fraction of gray matter in any given voxel as determined from tissue segmented imaging data (Hetherington et al., 1996; note that the concentrations of NAA and creatine in CSF are negligible). Based on mixed gray and white matter voxels measured from n = 10 group of controls (age range 21–52 years old, studies acquired from neocortical frontoparietal regions), a linear regression of NAA/Cr was developed as a function of fraction gray matter (fgm), that is, estimated NAA/Cr = 1.82–0.44*fgm. The significance of abnormality for a measurement from an arbitrary neocortical voxel was calculated from the difference between the expected versus observed NAA/Cr according to

$$\mathrm{Y(p<\alpha)cutoff=Y_{mean}(fgm)} \pm \mathrm{t_{\alpha}}*\mathrm{s_{y,\ fgmnew}}$$

where t_{α} is 1.65 ($n \geq 200$ points on the regression, α is 0.05 significance for one tailed *t*-test). The $s_{y,fgmnew}$ will vary depending on the new fgm value and represents the confidence interval for NAA/Cr al the new fgm value (Montgomery, 1991):

$$\mathrm{s_{y,\ fgmnew}=s_{y,x}}*\sqrt{1+\frac{1}{\mathrm{n}}+\frac{1}{n-1}*\left(\frac{\mathrm{fgmnew}-\overline{\mathrm{fgm}}}{\mathrm{se(fgm)}}\right)^2}$$

$s_{y,x}$ is the standard error of the estimate from the regression, n is the number of points in the regression. In this analysis, we used a one-tail *t*-test for significance because our hypothesis clearly anticipates abnormality with a decline in NAA/Cr.

Because hippocampal MRSI values are known to be different from neocortex (Vermathen et al., 2000; Choi & Frahm, 1999), these values were determined separately. In the anterior and posterior hippocampus, NAA/Cr values were measured in controls (n = 10) to be 1.21 ± 0.13 and 1.32 ± 0.10, respectively, with the cutoff for abnormality taken at two standard deviations low, at 0.95 and 1.12, respectively.

Results

Table 1 shows the demographic and clinical data for the 25 patients. In nine patients, there was preoperative MR-detected unilateral or asymmetric hippocampal abnormality. Another 10 patients had clinical MRI-detectable abnormalities such as periventricular heterotopia, bilateral symmetrical hippocampal abnormalities, or the residual scar from a remote hemorrhagic arteriovenous malformation. The remaining six patients had a negative clinical MRI. Of the 25 patients, n = 15 patients (i.e., most of the patients except those with clearly defined unilateral hippocampal onset and atrophy) underwent intracranial monitoring for seizure localization. The resulting contingency tables arc shown in Table 2, using letters A–F to describe the six possible groups. We approach the description of the results from the perspective of initial imaging-based localization.

It should be clearly acknowledged that the postsurgical outcome will always be modulated by the need to maintain adequate cognitive function. However, our goal in this work was to evaluate outcome based on concordance of the 7T MRSI abnormalities with the surgical resection, and for this, limitations caused by function are a separate issue.

Patients with MR-determined asymmetric hippocampal abnormality (n = 9)

As expected, all nine patients with asymmetric hippocampal abnormality and noninvasive consensus consistent with unilateral medial temporal lobe epilepsy (MTLE) fell into contingency group A, that is, class I (region of MRSI abnormality completely surgically resected) with I–III outcome (Table 2A). Two examples of data from this group (patients 1 and 4 from Table 1) are shown in Figure 1B,C, showing the characteristic anterior medial temporal lobe decline in NAA/Cr (for comparison Figure 1A shows data from a healthy control volunteer). These two examples are shown to demonstrate the variability in medial temporal lobe metabolic decline, with Figure 1B with injury unilaterally, although Figure 1C has injury throughout the ipsilateral hippocampus, with lesser abnormalities seen in the contralateral hippocampus.

Other patients with abnormal clinical imaging (including symmetric hippocampal atrophy [n = 10])

Ten patients had a variety of abnormalities detected by clinical imaging. As summarized in Table 2B, these patients fell into a variety of contingency groups. Excellent outcome was seen in six patients, characterized with discrete imaging abnormalities (e.g., mild increased signal on fluid-attenuated inversion recovery [FLAIR], graywhite blurring). Data from patient 14 (contingency group A) is shown in Figure 2, and shows the relatively restricted region of NAA/Cr spectroscopic abnormality, although there are mild adjacent abnormalities in NAA/Ch. One patient (no. 15, contingency group C) was not accurately detected by MRSI. This patient was studied with the larger voxel size (1.44 cc), and the NAA/Cr value from the known structural lesion in the left temporal lobe was 1.40. Although this value does not score as significantly abnormal, it should be noted that the contralateral homologous region has a value of 1.81, with the entire ipsilateral region being mildly decreased. With this study, it became clear that 1.44 cc sampling for neocortical epilepsy was likely to be inadequate and since then higher resolution studies have been acquired (21 patients), in this group, the volume of MRSI abnormality could be quite small, one or two voxels. Based on studies using a 0.64 cc voxel size, neocortical abnormalities were detected with NAA/Cr values of 1.13 ± 0.12, a mean fractional gray value of 0.8, this having a *t*-value of 2.42.

Of the remaining four patients (11, 16, 17, and 19) with poor outcomes, two had periventricular heterotopias on structural MRI (patients 16 and 17). The heterotopias or surrounding tissues did not show abnormalities in NAA/Cr (Fig. 3 shows patient 16 in this

region). Both of these patients had portions of the heterotopia resected in addition to subpial transections or resection of overlying cortex, but experienced poor outcomes and were classified as group F. The remaining two of this poor outcome group had dual pathology in the ipsilateral temporal lobe (no. 19), and likely bilateral MTLE (no. 11), both classified as group E, that is, the surgical resection did remove metabolically abnormal tissue, but the MRSI identified additional abnormality that was at least as severe and not resected. Of these four patients, the MRSI identified other candidate abnormalities; in three of these, the abnormality was located in the temporal lobe, which could be severe.

Patients with negative conventional imaging (n = 6)

Six patients had no clear imaging abnormalities and were initially poorly localized. Decision for the region of MRSI study was determined from semiology and scalp EEC, with these patients falling into contingency groups A (n = 1), B (n = 1), E (n = 2), and F (n = 2), see Table 2C. The group A patient 20 was determined after intracranial ERG localization to have MTL-onset seizures, identified accurately by MRSI. The group B patient 24 was determined with intracranial analysis to have left amygdalar onset, with MRSI showing wider limbic network abnormalities. The remaining five patients comprised two with childhood exposure to meningitis or encephalitis (21 and 22), and three with no clear etiology (23, 24, and 25). Figure 4 shows patient 21 (history of meningitis) with a poor outcome, showing multiple regions of metabolic abnormality.

3 × 2 Contingency table of total cohort

Table 2D summarizes ail of the contingency group data. Although it is clear that this is a small patient group, only one of the 25 patients analyzed fell into contingency groups C or D. It is possible that this “miss” (group C) was because of the larger voxel size used in that early study. Alternatively, it is possible that the severity of metabolic dysfunction of this lesion was small. Using a Fisher’s exact 3 × 2 contingency statistical test, the concordance between MRSI and surgical resection was significantly related to good outcome ($p < 0.001$). To calculate prediction values, we combined the contingency groups B + C (partial or no concordance between MRSI surgery, but with good outcome) and contingency groups E + F (partial or no concordance between MRSI surgery with poor outcome). When all 25 patients were included, the positive predictive value for the concordance of MRSI with good outcome was 100%, negative predictive value was 73%, sensitivity 82%, and specificity 100%. If the asymmetric hippocampal abnormality cases were omitted (based on a total of 16 patients), these parameters arc 100%, 73%, 62.5%, and 100%, respectively.

Discussion

These data are consistent with the view that regions with metabolic abnormalities are linked with seizure onset (Drzezga et al., 1999; Benedek et al., 2004; Shih et al., 2004) and abnormalities defined by NAA/Cr can provide pertinent information for prediction of short- to medium-term outcome in the surgical treatment of localization-related epilepsy. Specifically the resection of metabolically abnormal tissue was linked with good outcome, whereas resection of metabolically normal tissue was linked with poor outcome. Because this initial study used the MRSI to better define the metabolic anatomy of the surgical target region, these data provide useful estimates for outcome based on the extent of resection of the area of abnormal MRSI. It should be noted that the analyses of the neocortical patient data are based on control data (age range 21 – 52 years old) taken from frontoparietal neocortical regions. Given the possibility for normal variation in N AA/Cr based on age and lobe (Pouwels et al., 1999; Harada et al., 2001; Blüml et al., 2012), it is likely that greater sensitivity and specificity can be achieved by using more accurate control data. Nonetheless, these results suggest that MRSI may also provide more information and identification of

candidate regions of seizure onset. Clearly, for the goal of providing a wholly independent assessment of the localization-related epilepsy patient, MRSI data will be needed from the entire brain from a larger group of patients, Pathophysiologically, such data would also be of interest for better understanding as to what the MRSI says about the metabolic and network nature of the injury in epilepsy, for example, the postmeningitis patient 21, who showed multiple loci of depressed NAA/Cr (Fig. 4).

How does the MRSI vary between patients?

Although these early data cannot be extrapolated given the many varying pathologies seen in this group, it is pertinent to consider the variation and extent of metabolic abnormalities. Consistent with existing literature, the MTLE group was relatively easy to detect and was characterized by an apparent anterior-posterior gradient in the hippocampus of metabolic dysfunction (worst anteriorly) that was commonly bilateral (Vermathen et al., 2000; Hetherington et al., 2007), The extent of injury in the temporal lobe–onset patients was variable, with some showing relatively mild metabolic injury versus others with severe hippocampal involvement and wider spread involvement (see Fig. 1B,C). Although there is generally excellent predictability from structural MRI (here, n = 9 with asymmetric hippocampal abnormality), as is well known, MTLE can be present in patients without overt hippocampal atrophy (de Lanerolle et al., 2003). In this report, mere were an additional four of the n = 16 group (i.e., these without simple asymmetric hippocampal atrophy) who were found to show definite (n = 1) or likely (n = 3) metabolic dysfunction in the hippocampus consistent with MTLE (for a total of 13). It is also of interest to consider that the two patients with periventricular heterotopias (patients 16 and 17) did not display metabolic abnormality within the heterotopia directly or in the immediate surrounding tissue. Instead, distant MRSI abnormalities were seen with these two patients, suggesting the utility of MRSI to characterize the presence/absence of metabolic networks that may be informative toward localization and outcome.

To what extent can MRSI identify seizure onset?

Given the view that epileptogenic tissue is likely characterized by metabolic dysfunction and mitochondrial injury (Shih et al., 2004: Kann et al., 2005; Nishida et al., 2008), it is relevant to note that of the eight poor outcome patients (combining the contingency groups E and F), MRSI identified other regions of NAA/Cr abnormalities in at least seven. In three of these seven patients, intracranial LEG data were available from regions relatively close (within 2 cm) to several of these candidate regions (in patient 16, 22, and 24). However, in these three patients, the intracranial EEG data did not find specific seizure onset from these candidate regions. Although this may seem confusing, several factors may be contributing. First, NAA/Cr is a measure of metabolic dysfunction, and it is certainly possible that areas of dysfunction occur without being directly at the site of seizure onset. Second, these other regions may reflect the presence of a seizure or epilepsy network, for example, possibly as propagation paths. This is consistent with the extensive literature finding limbic-wide and extratemporal abnormalities in MTLE (Benedek et al., 2004: Mueller et al., 2011; Pan et al., 2012b), also seen in the MTLE patients from contingency group A. Finally, given the complex nature of this patient group, it is also possible that there are multiple loci of seizure onset where after resection of the initial seizure onset region, other (initially quiescent) aberrant regions may become active. Nonetheless, given our concordance between MRSI, resection, and outcome, it is clear that for the majority of our patients, finding and resecting the region with the most severe metabolic abnormality characterizes better patient outcome than resecting a metabolically normal region.

Advances in imaging technology are constructive for localization-related epilepsy

From an imaging perspective, the present data show that there is diversity among patients in the volumetric amount of metabolic dysfunction. Some patients show widespread abnormalities (e.g., patients 16, 18, and 19), whereas others have smaller regions of dysfunction (patients 13 and 14); therefore, with minimal a priori knowledge, there is need for excellent spectral quality and spatial resolution. Ongoing developments in ultra-high field MR arc realizing the anticipated advantage for SNR (Tkac et al., 2009; Hale et al., 2010), which is challenging specifically in terms of B0 field homogeneity and RF performance (Van de Moortele et al., 2005; Avdievich et al., 2009; Pan et al., 2012a). Recent progress in this area has made these large volume 7T high resolution studies possible, but it should also be noted that such technologic developments have immediate relevance for 3T or 4T, which is known to have similar (but somewhat milder) problems, especially in lower brain regions (Maudsley et al., 2010a,b). As a result, we arc optimistic that with continuing work, such studies will become feasible on clinical MR systems.

With continuing studies of this kind, we anticipate that the metabolic imaging may help to better understand The nature of the distributed injury in human epilepsy. More concretely, we also believe there to be specific value added with the MRSI study: that seizure localization can be improved and that better definition of the metabolic networks in epilepsy can hopefully improve outcomes from surgery.

Acknowledgments

Funding is gratefully acknowledged from the NIH EB011639, EB009871, NS054038, NIH EB 000473, and the Swebilius Foundation.

References

Avdievich NI, Pan JW, Baehring JM, Spencer DD, Hetherington HP. Short echo spectroscopic imaging of the human brain at 7T using transceiver arrays. Magn Reson Med. 2009; 62:17–25. [PubMed: 19365851]

Bates TE, Strangward M, Keelan J, Davey GP, Munro PM, Clark JB. Inhibition of *N*-acetylaspartate production: implications for 1H MRS studies in vivo. NeuroReport. 1996; 7:1397–1400. [PubMed: 8856684]

Benedek K, Juhász C, Muzik O, Chugani DC, Chugani HT. Metabolic changes of subcortical structures in intractable focal epilepsy. Epilepsia. 2004; 45:1100–1105. [PubMed: 15329075]

Blüml S, Wisnowski JL, Nelson MD Jr, Paquette L, Gilles FH, Kinney HC, Panigrahy A. Metabolic maturation of the human brain from birth through adolescence: insights from in vivo magnetic resonance spectroscopy. Cereb Cortex. 2012 Sep 5. [E-pub ahead of print].

Choi C, Frahm J. Localized proton MRS of the human hippocampus: metabolite concentrations and relaxation times. Magn Reson Med. 1999; 41:204–207. [PubMed: 10025631]

Connelly A, Jackson CD, Duncan JS, King MD, Gadian DC. Magnetic resonance spectroscopy in temporal lobe epilepsy. Neurology. 1994; 44:1411–1417. [PubMed: 8058140]

Connett RJ. Analysis of metabolic control: new insights using scaled creatine kinase model. Am J Physiol. 1988; 254:R949–R959. [PubMed: 2837918]

de Lanerolle NC, Kim JH, Williamson A, Spencer SS, Zaveri HP, Eid T, Spencer DD. A retrospective analysis of hippocampal pathology in human temporal lobe epilepsy: evidence for distinctive patient subcategories. Epilepsia. 2003; 44:677–687. [PubMed: 12752467]

Drzezga A, Arnold S, Minoshima S, Noachtar S, Szecsi J, Winkler P, Römer W, Tatsch K, Weber W, Bartenstein P. 18F-FDG PET studies in patients with extratemporal and temporal epilepsy: evaluation of an observer-independent analysis. J Nucl Med. 1999; 40:737–746. [PubMed: 10319744]

Goelman G, Liu S, Fleysher R, Fleysher L, Grossman RI, Gonen O. Chemical shift artifact reduction in Hadamard-encoded MR spectroscopic imaging at high (3T and 7T) magnetic fields. Magn Reson Med. 2007; 58:167–173. [PubMed: 17659608]

Guevara CA, Blain CR, Stahl D, Lythgoe DJ, Leigh PN, Barker GJ. Quantitative magnetic resonance spectroscopic imaging in Parkinson's disease, progressive supranuclear palsy and multiple system atrophy. Eur J Neurol. 2010; 17:1193–1202. [PubMed: 20402762]

Hale JR, Brookes MJ, Hall EL, Zumer JM, Stevenson CM, Francis ST, Morris PG. Comparison of functional connectivity in default mode and sensorimotor networks at 3 and 7T. MAGMA. 2010; 23:339–349. [PubMed: 20625794]

Harada M, Miyoshi H, Otsuka H, Nishitani H, Uno M. Multivariate analysis of regional metabolic differences in normal ageing on localised quantitative proton MR spectroscopy. Neuroradiology. 2001; 43:448–452. [PubMed: 11465755]

Hetherington HP, Pan JW, Mason GK, Adams D, Vaughn MJ, Twieg DB, Pohost CM. Quantitative 1H spectroscopic imaging of human brain at 4.1T using image segmentation. Magn Reson Med. 1996; 36:21–29. [PubMed: 8795016]

Hetherington HP, Kuzniecky RI, Vives K, Devinsky O, Pacia S, Luciano D, Vasquez B, Haut S, Spencer DD, Pan JW. A subcortical network of dysfunction in TLE measured by magnetic resonance spectroscopy. Neurology. 2007; 69:2256–2265. [PubMed: 18071146]

Hetherington HP, Avdievich NI, Kuznetsov AM, Pan JW. RF shimming for spectroscopic localization in the human brain at 7T. Magn Reson Med. 2010; 63:9–19. [PubMed: 19918903]

Inglese M, Spindler M, Babb JS, Sunenshine P, Law M, Gonen O. Field, coil, and echo-lime influence on sensitivity and reproducibility of brain proton MR spectroscopy. AJNR Am J Neuroradiol. 2006; 27:684–688. [PubMed: 16552016]

Kann O, Kovacs R, Njuntin M, Behrens CJ, Otahal J, Lehmann TN, Gabriel S, Heinemann U. Metabolic dysfunction during neuronal activation in the ex vivo hippocampus from chronic epileptic rats and humans. Brain. 2005; 128:2396–2407. [PubMed: 15958506]

Kuzniecky R, Hetherington H, Pan JW, Hugg J, Palmer C, Gilliam E, Faught E, Morawetz R. Proton spectroscopic imaging at 4.1 tesla in patients with malformations of cortical development and epilepsy. Neurology. 1997; 48:1018–1024. [PubMed: 9109893]

Maudsley AA, Domenig C, Ramsay RE, Bowen BC. Application of volumetric MR spectroscopic imaging for localization of neocortical epilepsy. Epilepsy Res. 2010a; 88:127–138. [PubMed: 19926450]

Maudsley AA, Domenig C, Sheriff S. Reproducibility of serial whole-brain MR spectroscopic imaging. NMR Biomed. 2010b; 23:251–256. [PubMed: 19777506]

Montgomery, D. Design and analysis of experiments. 3rd ed.. New York: Wiley and Sons; 1991. p. 484-490.

Mueller SG, Ebel A, Barakos J, Scanlon C, Cheong I, Finlay D, Garcia P, Weiner MW, Laxer KD. Widespread extrahippocampal NAA/(Cr + Cho) abnormalities in TLE with and without mesial temporal sclerosis. J Neurol. 2011; 258:603–612. [PubMed: 20976465]

Muñoz Maniega S, Cvoro V, Chappell FM, Armitage PA, Marshall I, Bastin ME, Wardlaw JM. Changes in NAA and lactate following ischemic stroke: a serial MR spectroscopic imaging study. Neurology. 2008; 71:1993–1999. [PubMed: 19064881]

Nishida M, Juhasz C, Sood S, Chugani HT, Asano E. Cortical glucose metabolism positively correlates with gamma oscillations in nonlesional focal epilepsy. Neuroimage. 2008; 42:1275–1284. [PubMed: 18652902]

Pan JW, Takahashi K. Inter-dependence of *N*-acetyl aspartate and high energy phosphates in human brain. Ann Neurol. 2005; 57:92–97. [PubMed: 15546136]

Pan JW, Lo KM, Hetherington HP. Role of high degree and order B0 shimming for spectroscopic imaging at 7T. Magn Reson Med. 2012a; 68:1007–1017. [PubMed: 22213108]

Pan JW, Spencer DD, Kuzniecky R, Duckrow RB, Hetherington H, Spencer SS. Metabolic networks in epilepsy by MR spectroscopic imaging. Acta Neurol Scand. 2012b; 126:411–420. [PubMed: 22574807]

Pouwels PJ, Brockmann K, Kruse B, Wilken B, Wick M, Hanefeld F, Frahm J. Regional age dependence of human brain metabolites from infancy to adulthood as detected by quantitative localized proton MRS. Pediatr Res. 1999; 46:474–485. [PubMed: 10509371]

Rooney WD, Johnson G, Li X, Cohen ER, Kim SG, Ugurbil K, Springer CS Jr. Magnetic field and tissue dependencies of human brain longitudinal 1H2O relaxation in vivo. Magn Reson Med. 2007; 57:308–318. [PubMed: 17260370]

Shih JJ, Weisend MP, Lewine J, Sanders J, Dermon J, Lee R. Areas of interietal spiking are associated with metabolic dysfunction in MRI-negative temporal lobe epilepsy. Epilepsia. 2004; 45:223–229. [PubMed: 15009223]

Suhy J, Rooney WD, Goodkin DE, Capizzano AA, Soher BJ, Maudsley AA, Waubant E, Andersson PB, Weiner MW. 1H MRSI comparison of white matter and lesions in primary progressive and relapsing-remitting MS. Mult Scler. 2000; 6:148–155. [PubMed: 10871825]

Tkác I, Oz G, Adriany G, Uğurbil K, Gruetter R. In vivo 1H NMR spectroscopy of the human brain at high magnetic fields: metabolite quantification at 4T vs. 7T. Magn Reson Med. 2009; 62:868–879. [PubMed: 19591201]

Van de Moortele PF, Akgun C, Adriany G, Moeller S, Ritter J, Collins CM, Smith MB, Vaughan JT, Uğurbi K. B(1) destructive interferences and spatial phase patterns al 7T with a head transceiver array coil. Magn Reson Med. 2005; 54:1503–1518. [PubMed: 16270333]

Vaughan JT, Garwood M, Collins CM, Liu W, DelaBarre L, Adriany G, Andersen P, Merkle H, Goebel R, Smith MB, Ugurbil K. 7T vs. 4T: RF power, homogeneity, and signal-to-noise comparison in head images. Magn Reson Med. 2001; 46:24–30. [PubMed: 11443707]

Vermathen P, Laxer KD, Matson GB, Wiener MW. Hippocampal structures: antero-posterior NAA differences in patients with epilepsy and control subjects as shown with proton MR spectroscopic imaging. Radiology. 2000; 214:403–410. [PubMed: 10671587]

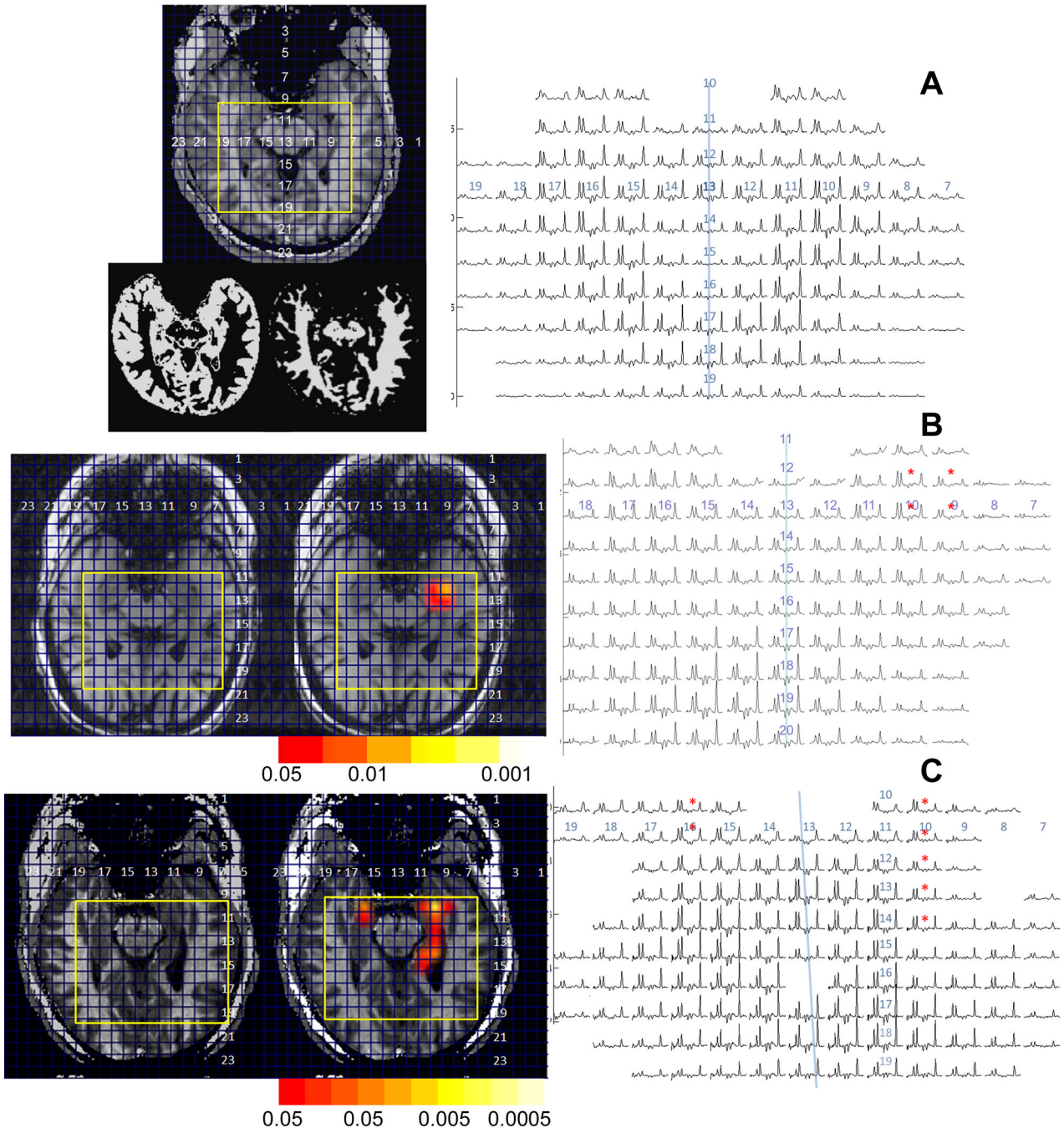

Figure 1.

Medial temporal lobe data (scout, spectra) from three volunteers, (**A**) control; (**B, C**) MTL patients and 4. For the two epilepsy patients, overlays are shown with color bars indicating level of significance overlaid on the anatomic scouts. The study from (**B**) shows less injury than (**C**). In the spectra, asterisks highlight the areas with abnormal NAA/Cr. In (**A**), results of gray and white matter tissue segmentation are also shown. The blue line approximately indicates the interhemispheric fissure. On both the scouts and spectra, corresponding row and column numbers are shown, with the yellow rectangles indicating die boundaries of the shown spectroscopic imaging data.

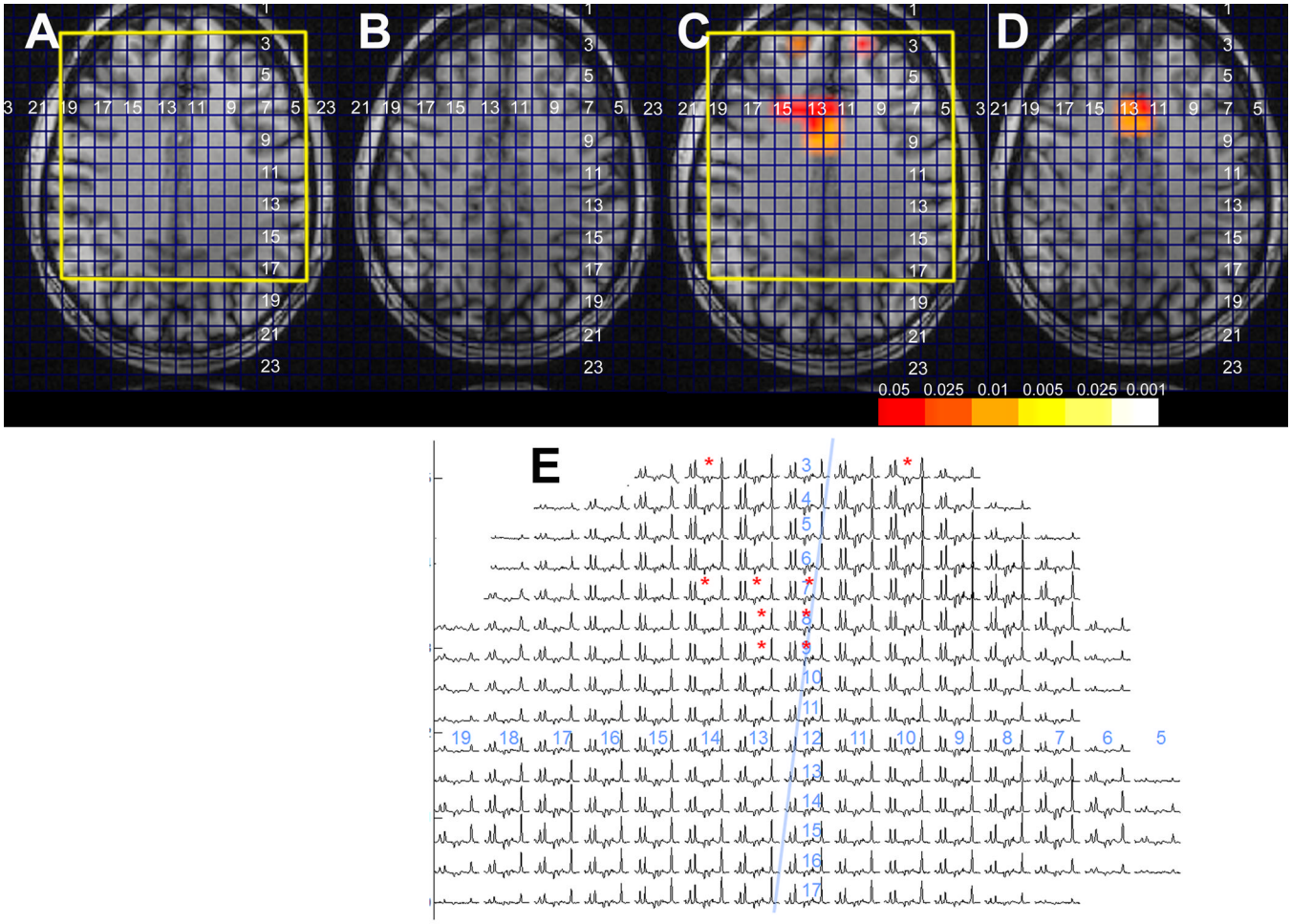

Figure 2.

Frontal lobe MRSI data from patient 4, showing the small parasagittal R. frontal lobe NA/Cr decline. (**A, B**) Scout images from two adjacent slices, (**C, D**) corresponding spectroscopic imaging overlays from the two slices, and (**E**) spectra from the more inferior slice (matching **A, C**). This patient underwent right frontal lobectomy including the involved area and has become seizure free with outcome class I. Pathology showed hyaline astrocytopathy of cortex. Unfortunately no postoperative imaging data are available.

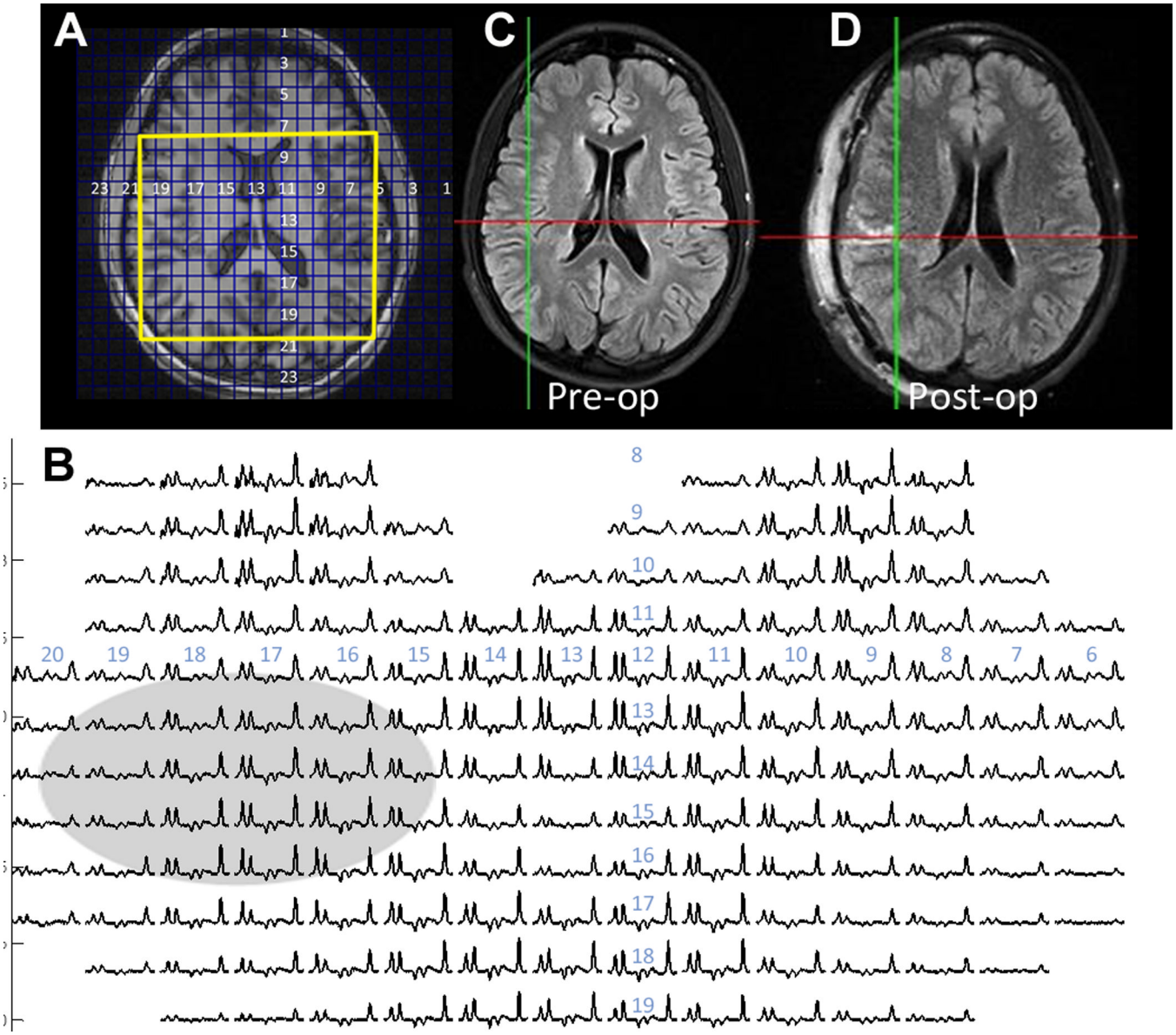

Figure 3.

Frontotemporal MRSI data from patient 6, who had a right periventricular nodular heterotopia (arrow). The scout (**A**), spectra (**B**), and clinical (**C, D**) preoperative and postoperative images are shown. The NA/Cr values from the spectra overlapping the heterotopia are within normal range when corrected for gray matter content. Additional NA/Cr abnormality was detected in the right medial temporal lobe of this patient (not shown). This patient underwent partial resection of heterotopia with subpial transections in overlying cortex, limited by visual tracts, with outcome class V.

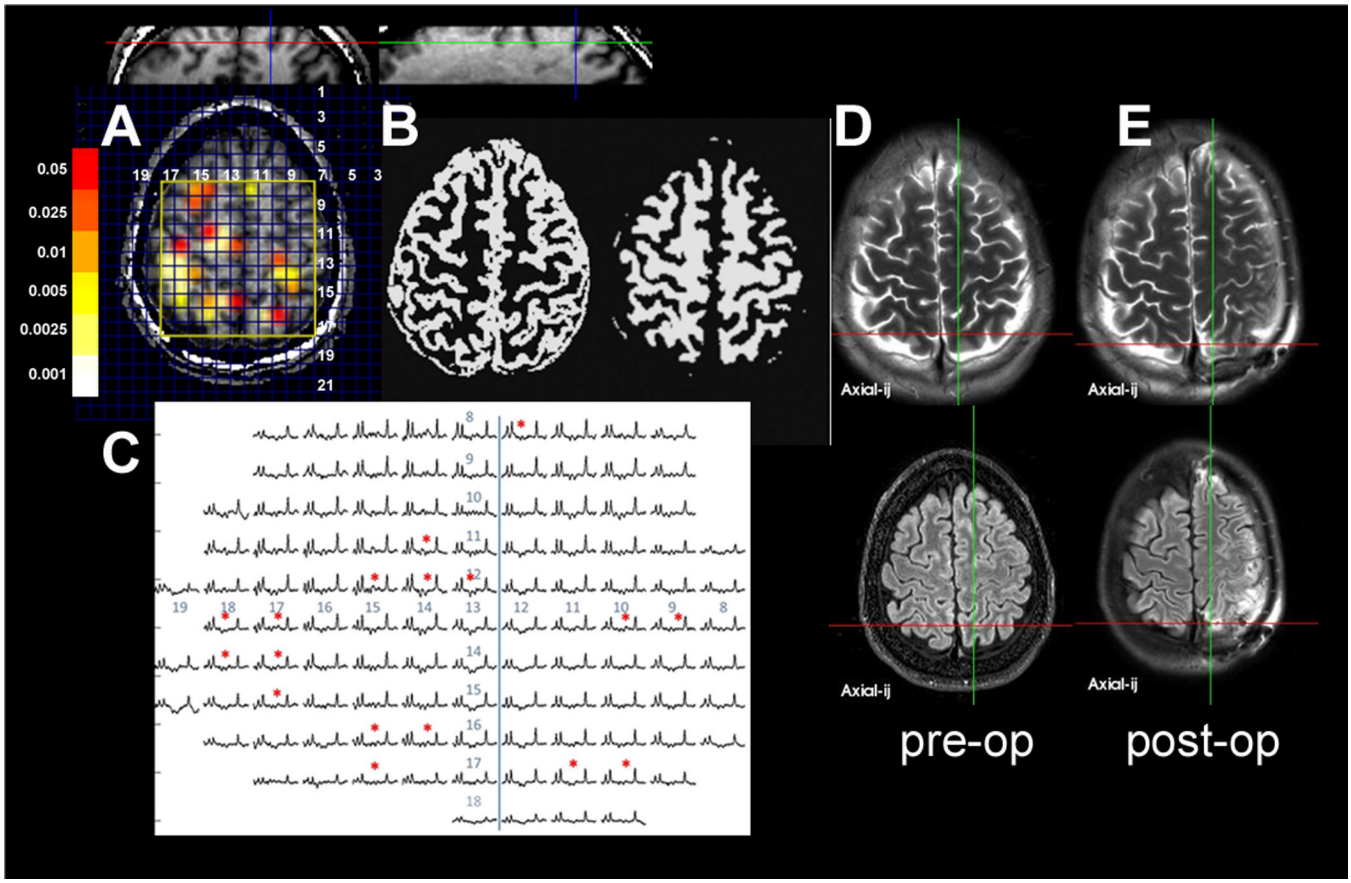

Figure 4.

Data from patient 2, showing the (**A**) scout with overlay (coronal and sagittal also shown). (**B**) tissue segmented data spectra, (**C**) spectra, and (**D, E**) preoperative and postoperative clinical imaging data. There are multiple regions of NA/Cr abnormality seen in both hemispheres. This patient with a history of childhood meningitis had a semiology that was entirely based in the left hemisphere; therefore, no intracranial recording was obtained from the right hemisphere. After precuneus resection on the left in the region of the left posterior MRSI abnormality, the patient was seizure free for approximately 3 months, but then relapsed as outcome class IV.

Table 1

Patient details and classifications[a]

ID	Sex	Age at study	Years of epilepsy	Consensus localization	MRI abn	PET abn	MRSI abn	P3?	Surgical procedure	Pathology	Outcome length and class	Contingency class
Patients with MTLE, MRI-Identified												
	F	52	5	L MTL	L HA	L anterolat temp	L MTL	No	L AMTL	L MTS	I, 6 months	A
2	F	5	34	R MTL	R HA	R inf par and temp	R MTL	No	R AMTL	R MTS	I, 2.5 years	A
3	F	9	4	L MTL	VP shunt, L Hc FLAIR	L med + lat temp	L MTL worse than R	No	L AMTL	L MTS CA, mild loss CA3	II, 3 years	A
4	F	29	4	L MTL	L HA	L inferolat temp	L MTL	No	L AMTL	L MTS	I, 2 years	A
5	M	35	22	R MTL	R HA	R MTL	R MTL	No	R AMTL	R MTS	I, .5 years	A
6	M	45	25	L MTL	Bi HAL worse than R	L lat temp	L MTL	No	L AMTL	L HS with heterotopic and dysplastic n	III, year 7 months	A
7	F	43	0	R temp: cavernoma s/p resection	Resection cavity, R ant temp lobe	R ant temp	R ant MTL	No	R ant temp pole incl amy and residual scar	N/A	I, 2 years	A
8	F	5	6	L MTL	L Hc cavernoma	L med temp	L MTL	No	L AMTL	Cavernoma	I, years	A
9	F	58	8	L MTL	L Hc	Negative	L ant MTL	No	L AMTL	CA3, CA4 neuron loss, some wm n	I, 2.5 years	A
0	F	42	20	R MTL	B MTLR worse than L	L temp	R MTL worse than L MTL	Yes	R AMTL	CA neuroral loss, some wm n	I, 3 years	A
	M	27	6	R MTL	R temp post-surg changes	N/A	Bi MTL	No	R AMTL (s/p earlier R STG)	CA neuroral loss; reactive gliosis	IV, 3 years	E
Patients with NON-MTLE with identified (MRI or PET) lesion												
2	F	30	9	R fr	R sup fr FLAIR	Negative	R sup fr sulc	Yes	R sup-med fr back to SMA	Reactive gliosis, mild incrs wm neurons	I, 2 years	A
3	F	25	22	R sup fr gy	R sup fr gy FLAIR	L temp anterior	R sup fr gy	Yes	R sup fr gy and lateral	FCD with balloon cells Taylor type	I, 3.5 years	A
4	M	7	8+	R fr	Negative	R fr	R med sup fr gy	Yes	R fr	Hyaline astrocytopathy of cortex	I, year	A
5	M	8	5	L fr posterior	L inf fr gy FLAIR	Negative	Not significantly abnl	Yes	L post fr dysplasia	Cortical dysplasia	I, 3.5 years	C

ID	Sex	Age at study	Years of epilepsy	Consensus localization	MRI abn	PET abn	MRSI abn	P3?	Surgical procedure	Pathology	Outcome length and class	Contingency class
6	M	30	9	Diffuse onset R parietal-temp	R perivent heterotopia R trigone	R ant temporal	R MTL	Yes	Partial resection of dysplasia, par-temp MST (limited by visual field)	Normal cortex	IV, 2.5 years	F
7	F	2	0	Prob onset over nodule	R perivent heterotopia	N/A	R sup fr gy	Yes	R nodule; cortical R fr and par face	Reactive astrocytes	V, year 4 months	F
8	M	20	5	AVM rupture L temp-par	Cystic en cephalomalacia L temp-par	Extensive post L temp-par	Lesion, also mid occgy	Yes	9.5 cm L lat temp, MST post-fr and par	Gliosis, c/w remote is chemia	II, 5 months	B
9	F	34	2	L temp pole	L temp pole FLAIR	Negative	L MTL and STG-pole	Yes	Tallored L temp pole, limited by cogn function	Non specific: subacute infarction and chronic vascular changes	V,4 months	E
Patients with NEGATIVE STRUCTURAL imaging												
20	F	25	4	L MTL, lat temp	Negative	R lat inf temp	R MTL	Yes	R AMTL with 5 cm lateral temp	Reactive gliosis, wm n; in Hc also with mild n loss	I, 2.5 years	A
2	F	53	43	L motor-sensory	Negative	Negative	L sup par lob-precuneus; R sup fr gy; R post-central sulc	Yes	L precuneus, MST L motor sensory and sup par lob	Reactive gliosis, scattered wm n	IV, 7 months	E
22	F	24	4	L temp-occ with L Hc; R MTL	Negative	Negative	L post MTL and med occ; mild R post MTL	Yes	Topectomy of contacts I 5–8 post MTG-occipital	Mild incrs wm neurons	V, year 4 months	F
23	F	29	5	Parasag R fr motor	Negative	R temp, lat	Mild R cing gy	Yes	R pre-frontal to SMA	Reactive gliosis, mild incrs wm n	IV, .5 years	F
24	F	26	25	L amyg	Negative	R temp, med	L ins, R ant MTL	Yes	L amygdala	Rare heterotopic n	II, 4 months	B
25	F	44	29	L MTL	Negative	R temp, lat	B MTL	Yes	L AMTL	Mlld gliosis	IV, 3 years	E

Temp, temporal; fr, frontal; occ, occipital; par, parietal; amyg, amygdala; ins, insula; cing, cingulate; MTG, middle temporal gyrus; STG, superior temporal gyrus; Hc, hippocampus; periven, periventricular; SMA, stpplementary motor area; gy, gyrus; HA, hippocampal atrophy; MST, multiple subpial transections; AMTL, anterior medial temporal lobectomy; cogn, cognitive; VP, ventriculoperitoneal; FCD, focal cortical dysplasia; MTS, mesial temporal sclerosis; HS, hippocampal sclerosis; wm, white matter; n, neurons.

[a] All localization and surgical decisions made by expert review and consensus opinion, making use of intracranial data if available.

Table 2

3 × 2 contingency tables for n = 25 patients

A:N = 9 Asymmetric HA only		
	Outcome: I-III	**Outcome IV-VI**
Complete concordance	A:9	D:0
Partial concordance	B:0	E:0
Discordant	C:0	F:0
B:N = 10 Abnormal clinical MRI or PET (other than asymmetric HA)		
	Outcome: I-III	Outcome IV-VI
Complete concordance	A:4	D:0
Partial concordance	B:	E:2
Discordant	C:1	F:2
C:N = 6 Negative clinical imaging		
	Outcome: I-III	Outcome IV-VI
Complete concordance	A:	D:0
Partial concordance	B:	E:2
Discordant	C:0	F:2
D:All 25 patients: $p < 0.00$ significant correlation between the two outcome groups and concordance, $\chi^2 = 5.2$		
	Outcome: I-III	Outcome IV-VI
Complete concordance	A: 4	D:0
Partial concordance	B:2	E:4
Discordant	C:1	F:4

Based on all 25 patients and combining contingency groups B+C and E+ F, the positive predictive value for the concordance of MRSI (either complete concordance vs. partial or no concordance) with surgical resection for good outcome is 00%; negative predictive value 73%, sensitivity 82% and specificity 100%.